Nuclear Mathematical and Computational Sciences: A Century in Review, A Century Anew
Gatlinburg, Tennessee, April 6-11, 2003, on CD-ROM, American Nuclear Society, LaGrange Park, IL (2003)

NEUTRON CAPTURE OF ^{232}Th IN THE UNRESOLVED RESONANCE REGION – DATA CORRECTIONS AND ANALYSIS

A. Lukyanov, N. Koyumdjieva, N. Janeva, K. Volev
Institute for Nuclear Research and Nuclear Energy,
Blvd. Tzarigradsko Shaussee 72, 1784 Sofia, Bulgaria
pripesho@inrne.bas.bg

A. Brusegan, P. Schillebeeckx, G. Lobo, F. Corvi
EC-JRC Institute for Reference Materials and Measurements,
2440 Geel, Belgium
peter.schillebeeckx@irmm.jrc.be

ABSTRACT

An analytical solution to calculate the self-shielding and multiple scattering effects for the analysis of neutron capture cross-section data is described. The solution is valid for targets with a radius much larger than the thickness and a cylindrical neutron beam perpendicular to the surface of the target. In these conditions, the Flat Flux and Narrow Resonance approximations are applied. Average resonance parameters for ^{232}Th, in the unresolved resonance region, are estimated from recent experimental capture data obtained at GELINA. The resonance averaged cross sections and other functionals (cross section moments, self-shielding factors, transmission functions) are deduced from a statistical model. In the model the cross-section is parameterised by the Reich-Moore approximation of R-matrix theory and the characteristic function F of the R-matrix elements distribution is introduced.

Key Words: unresolved resonance region, self-shielding, multiple scattering, average resonance parameters, ^{232}Th

1. INTRODUCTION

To deduce average resonance parameters from experimental capture data in the unresolved resonance region (URR) one has to account for self-shielding and multiple scattering effects. This is the classical problem of neutron transport in a flat sample with self-shielding [1-4]. In the first part of the paper, an analytical solution to calculate the corresponding correction factors is given. The solution is given for a target disk with a radius much larger than the thickness and a cylindrical neutron beam perpendicular to its surface. In these conditions, the Flat Flux (FF) and Narrow Resonance (NR) approximations are applied. Self-shielding and multiple scattering corrections for ^{232}Th capture data are calculated. The results are compared with results from Monte Carlo calculations [5,6].

In the second part of the paper a statistical model [7], used to deduce average resonance parameters from experimental data in the unresolved resonance region, is presented. In a

previous paper [8] the model has been validated using experimental data for ^{56}Fe and ^{238}U in the resolved resonance region. In this paper we deduce average resonance parameters in the URR for ^{232}Th from recent average capture data obtained at GELINA [9]. The results are verified by a comparison with data obtained from self-indication measurements [10].

2. SELF-SHIELDING IN RESONANCE NEUTRON CAPTURE EXPERIMENTS

An accurate evaluation of neutron capture cross section data, obtained from high-precision time-of-flight experiments, depends strongly on the experimental conditions in the energy region of interest. Besides corrections related to normalisation, background conditions, Doppler and resolution broadening, one also has to account for self-shielding and multiple-scattering effects. For relatively thick targets, the interpretation of capture yields becomes a complex process. This is due to:

- the resonant structure of neutron cross sections,
- the dependency of the neutron energy after scattering on both the scattering angle and the thermal motion of the scattering nucleus,
- the possibility that a neutron may undergo a considerable number of collisions before final absorption or escape.

In multilevel resonance analysis codes, such as REFIT [11] and SAMMY [12], self-shielding and multiple scattering corrections are based on analytical solutions. In principle, the best way to approach the problem is by Monte Carlo simulations. Such simulations can be performed by the following codes: SESH [6], SAMSMC [13] or MCNP [5]. However, using MCNP one has to be careful since sampling of the cross-section is based on point wise data.

In this paper an analytical solution to the problem, similar to Dressner's approach in Ref. [14], is described. The solution is valid for targets with a radius R much larger than the thickness d and a cylindrical neutron beam perpendicular to the surface of the target. The total number of neutron collisions in the sample at energy E per time unit can be presented as [2,4]:

$$F(E) = J(E)(1 - e^{-d\Sigma(E)}) + P(E)\int dE' \frac{\Sigma_s}{\Sigma}(E')F(E')W(E' \to E), \qquad (1)$$

where $J(E)$ is the neutron intensity, $P(E)$ is the collision probability of neutrons with energy E, and $W(E' \to E)$ denotes the energy distribution of scattered neutrons [4]. The macroscopic elastic and total cross-section are given by Σ_s and Σ respectively. Equation 1 represents the collision probability as a sum of two terms:

- the first contribution is due to collisions of neutrons which had no previous interactions
- the second results from neutrons that are slowed down in the sample.

The effect of neutron flux reduction at first collision is important for the self-shielding. The contribution of slowing down neutrons is usually not large (≤ 10% for relatively thin targets). Therefore, for estimation purposes some assumptions can be used to simplify the calculations:

- in the Flat Flux approximation [2,4] the collision probability can be expressed as:

$$P(E) \approx P_0[\bar{l}\Sigma(E)] = 1 - \frac{\overline{(1-e^{-l\Sigma})}}{\bar{l}\Sigma}, \qquad (2)$$

where the averaging is made over all possible lengths in the sample between arbitrary points of the surface ($l = \left|\vec{r}_s - \vec{r}'_s\right|$).

- when the resonances are well separated and their widths are small compared to the neutron energy loss by elastic scattering the Narrow Resonance Approximation (NR) can be applied, and the results can be presented in an analytical form [2].

2.1 Isolated Resonance

Let us consider a resonance at energy E_l. At energies $E \approx E_l$ the integral term in the equation for $F(E)$ (Eq. 1) is determined by the solution at off-resonance energies F_0. Here the cross section changes smoothly with the energy and approaches the potential scattering $\Sigma \approx \Sigma_p$. Assuming a constant neutron intensity, $F_0(E)$ does not depend from the energy and according to equation (1) we have:

$$F_0 = J(E)\, f_0(d\Sigma_p), \quad f_0(d\Sigma_p) = (1 - e^{-d\Sigma_p}) \big/ (1 - P_0(\bar{l}\Sigma_p)). \qquad (3)$$

In the NR-approximation, the function $F(E)$ at resonance energies can be represented as [2]:

$$F(E) = J\langle (1 - e^{-d\Sigma(E)}) + f_0(d\Sigma_p) P_0[\bar{l}\Sigma(E)] \rangle, \qquad (4)$$

where the last term is accounting for neutrons slowing down in the sample. Neglecting any resolution broadening effect, the absorption intensity around the resonance energy E_l becomes:

$$N_{al}(d) = \int_{\Delta E_l} \frac{\Sigma_a(E)}{\Sigma(E)} F(E) dE. \qquad (5)$$

with $\Sigma_a(E)$ the macroscopic absorption cross-section. The ratio of $N_{al}(d)$ for a sample with finite thickness d to the corresponding intensity for an infinite thin target ($d \to 0$) determines the self-shielding coefficient $C^l(d)$:

$$C^l(d) = \int_{\Delta E_l} \frac{\Sigma_a(E)}{\Sigma(E)} F(E) dE \Big/ d \int_{\Lambda E_l} J\Sigma_a(E) dE = C_1^l(d) + C_2^l(d) \qquad (6).$$

The effect due to first collisions is accounted for in the coefficient C_1^l:

$$C_1^l(d) = \int_{\Delta E_l} \frac{\Sigma_a(E)}{\Sigma(E)}\left(1 - e^{-d\Sigma(E)}\right)dE \Big/ d \int_{\Delta E_l} \Sigma_a(E)dE \qquad (7).$$

The coefficient $C_2^l = C^l - C_1^l$, related to the neutrons slowing down in the sample, becomes:

$$C_2^l(d) = f_0(d\Sigma_p) \int_{\Delta E_l} \frac{\Sigma_a(E)}{\Sigma(E)} P_0\left[\bar{l}\,\Sigma(E)\right]dE \Big/ d \int_{\Delta E_l} \Sigma_a(E)dE\,, \qquad (8)$$

where $P_0(x)$ can be approximated by (see Par. 2.2):

$$P_0(x) = \frac{1}{n}\sum_{i=1}^{n} \frac{a_i x}{1 + b_i x}, \qquad (x = d\Sigma) \qquad (9).$$

Using the SLBW approximation the macroscopic absorption and total cross-section becomes:

$$\Sigma_a(E) = \Sigma_{0l}\left(\Gamma_{al}/\Gamma_l\right)\ \Psi\left(2\frac{E_l - E}{\Gamma_l},\ \frac{\Gamma_l}{2\Delta}\right),$$

$$\Sigma(E) = \Sigma_p + \Sigma_{0l}\left[(\cos 2j)\Psi\left(2\frac{E_l - E}{\Gamma_l},\ \frac{\Gamma_l}{2\Delta}\right) - (\sin 2j)\mathrm{X}\left(2\frac{E_l - E}{\Gamma_l},\ \frac{\Gamma_l}{2\Delta}\right)\right], \qquad (10)$$

with Σ_p the macroscopic potential scattering cross-section, Γ_{al} and Γ_l the absorption and total resonance width resp., and $\Sigma_{0l}(E) = r\ 4p\ k^{-2}\ g(J)\,\Gamma_{nl}(E)/\Gamma_l(E)$ resonance peak cross-section. The Doppler broadening Δ is taken into account by means of the Voigt profiles through the resonance shape functions $\Psi(x,y)$ and $\mathrm{X}(x,y)$. The resonance integrals can be obtained from:

$$\int_{\Delta E_l} \Sigma_a(E)dE = p\ \Sigma_{0l}\ \Gamma_{al}\ /2 = A_l\,,$$

$$\int_{\Delta E_l} \frac{\Sigma_a(E)}{\Sigma(E)}\ \frac{a_i \Sigma d}{b_i \Sigma d + 1}\,dE = A_l\ \frac{a_i d}{1 + b_i d\ \Sigma_p}\ K\left(h_l^i, V_l, j\right), \qquad (11)$$

where the self-shielding coefficient for the effective resonance is defined as:

$$K\left(h_l^i, V_l, j\right) = \frac{1}{p}\int_{-\infty}^{\infty} \frac{\Psi(x,V_l)dx}{1 + h_l^i\left[\cos 2j\,\Psi(x,V_l) - \sin 2j\,\mathrm{X}(x,V_l)\right]} \qquad (12)$$

with $V_l = \Gamma_l/2\Delta$ and

$$h_l^i = b_i \sum_{0l} d \Big/ \left(1 + b_i d \sum_p\right) \tag{13}$$

On Fig.1 we illustrate the influence of Doppler broadening on the self-shielding coefficient $K\left(h_l^i, V_l, j = 0\right)$ as a function of the parameter h, related to the relative amplitude of the resonant structure. Fig.1 reveals that for a given Doppler broadening the largest contribution to the coefficient K results from relative weak resonances. In the case of strong resonances the coefficient tends to 1.

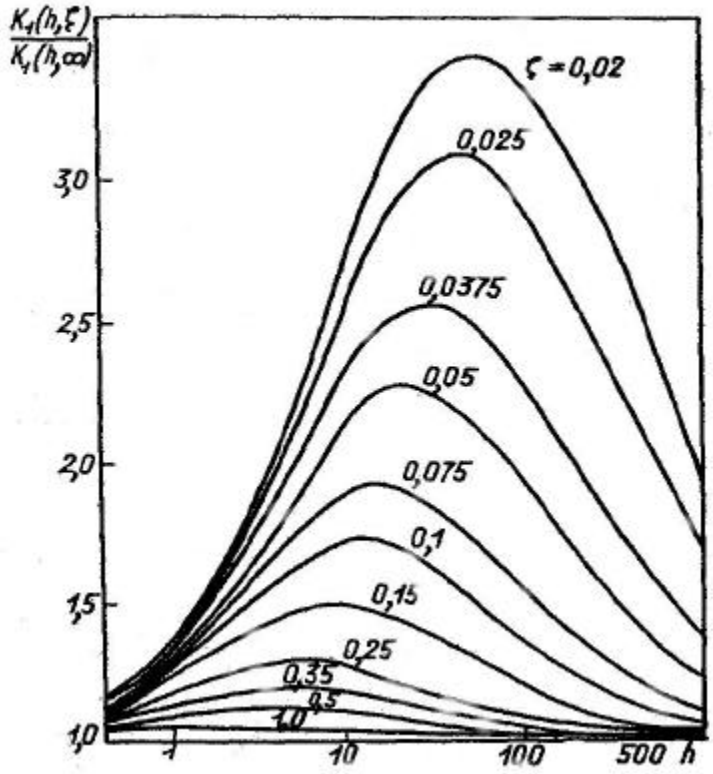

Figure 1. Influence of Doppler broadening in resonance integrals.

Finally, the coefficient C_2 can be calculated by:

$$C_2^l(d) = f_0(d\Sigma_p)\frac{1}{n\sum_{0l} d}\sum_{i=1}^{n}\frac{a_i}{b_i}\ h_l^i K\left(h_l^i, V_l, j\right). \tag{14}$$

The behaviour of $C_2^l\left(d\Sigma_p, \Sigma_0/\Sigma_p\right)$ as a function of Σ_0/Σ_p for different temperatures is presented in Fig. 2.

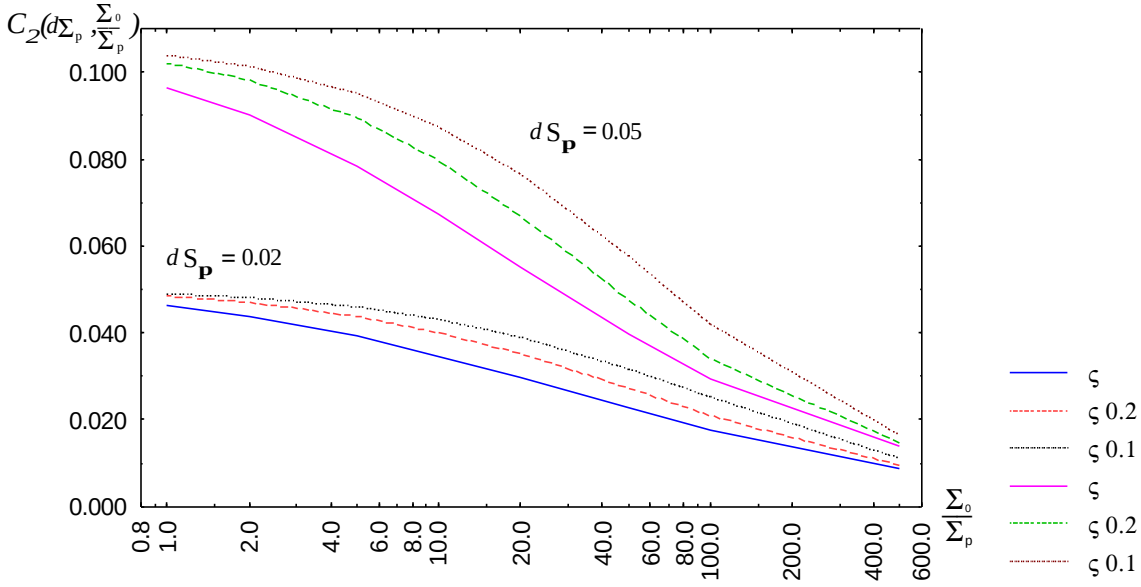

Figure 2. Coefficients $C_2(dS_p, S_0/S_p)$ for different temperatures.

2.2 Approximations

In practical applications, for large R/d ratios (>10), we can use the collision probability P_0 for an infinite plane layer [1,14]:

$$P_0(x) = 1 - \frac{1}{x}\left[0.5 - E_3(x)\right], \quad (x = d\Sigma), \tag{15}$$

where $E_3(x)$ is the exponential integral [15]. This expression can be used to verify approximations based on Eq. 9 (Table 1). The most simple one, the Wigner approximation:

$$P_W(x) \approx \frac{2x}{1+2x} \quad , \tag{16}$$

results in deviation up to 15%. Applying Dressner's expression:

$$P_D(x) \approx \frac{1}{2}\left(\frac{x}{1+x} + \frac{3x}{1+3x}\right) \quad , \tag{17}$$

the deviations with Eq. 15 are smaller. For $x > 0.1$ they are less than 5 %. However, for $x < 0.1$ the deviations increase rapidly. From a fit of data resulting from Eq. 15, we obtain the following parameters for the application of Eq. 9:

$$P(x) \approx \frac{1}{2}\left(\frac{3.374x}{1+25.21x} + \frac{2.626x}{1+1.41x}\right) \quad , \tag{18}$$

In the whole region of interest, values of P calculated with Eq. 18 are in reasonable agreement with those given by P_0 (see Table 1).

Table 1. Rational approximations of P(x).

x	P_0 (Eq. 15)	P_W (Eq. 16)	P_D (Eq. 17)	P (Eq. 18)
0.01	0.0277	0.020	0.020	0.026
0.05	0.0984	0.091	0.090	0.097
0.10	0.1629	0.167	0.161	0.163
0.50	0.4432	0.500	0.467	0.447
1.00	0.6097	0.667	0.625	0.610
2.00	0.7651	0.800	0.762	0.754
5.00	0.9002	0.909	0.885	0.883

Tabulated and plotted values for the self-shielding coefficients $K(h,V,j)$ can be found in several publications [2-4,16]. For $V_l > 1$ and no Doppler broadening, a simple approximation, in good agreement (within 3-4 %) with the results of exact calculations, is

$$K(h,V,j) = \left(1 + \frac{h}{1+d}\cos^2 j\right)^{-1/2}\left(1 - \frac{h}{1+d}\sin^2 j\right)^{-1/2}, \qquad (19)$$

where:

$$d^{-1} = V\left\{2{,}5 + 2V + \left[(1 + h\cos 2j)V\right]^{(0{,}1+V)/(0{,}12+V)}\right\}.$$

For relatively thin and homogenous samples ($d\Sigma_p << 1$), the effect of the resonance and potential scattering interference can be neglected ($j = 0$). In these conditions Eq. 19 becomes the solution proposed by L. Dresner (Ref. 2 Eq. 57).

2.3 Unresolved Resonances

In the unresolved resonance region, we assume that the resonances are relatively well separated and narrow compared to the mean elastic scattering energy loss. The self-shielding correction factor in the unresolved region can be deduced form Eq. 14, together with the statistical distribution of resonance parameters. For a given reaction channel, with total moment J and defined parity, the coefficient $C_2^J(d,E)$ may be written as:

$$C_2^J(d,E) = \bar{f}_0 \frac{1}{nd\,\bar{\bar{\Sigma}}_{0J}} \sum_{i=1}^{n} \frac{a_i}{b_i}\, \bar{h}_J^i\; K\left(\bar{h}_J^i, V_J, j\right) \mathrm{X}\left(\bar{h}_J^i\right) / \mathrm{X}(0) \qquad (20)$$

with $V_J = \overline{\Gamma}_J(E)/2\Delta(E)$ and $\overline{\Sigma}_{0J}(E)$ the total peak cross section for a "mean resonance" in the interval $\left[E - \frac{\Delta E}{2}, \mathrm{E} + \frac{\Delta \mathrm{E}}{2}\right]$ with average parameters $\overline{\Gamma}_{nJ}(E)$ and $\overline{\Gamma}_J(E)$. The function $\mathrm{X}(h)$ accounts for the resonance parameter fluctuations in averaging (14) and is calculated by using Porter-Thomas statistical distributions. The results for non-fissile nuclei are presented in Fig. 3. It follows that for values of the parameter $h < 10$, the ratios $\mathrm{X}(h)/\mathrm{X}(0)$ are very close to one. Consequently, even when strong fluctuations of the widths occur, as in the case of weak resonances, the influence of the fluctuations is small.

For different reaction channels with different J, the total self-shielding coefficient is the sum of the contributions of the different channels:

$$C_2(d,E) = \sum_J \langle s_{aJ}(E)\rangle C_2^J(d,E)/\langle s_a(E)\rangle, \tag{21}$$

where the brackets for $< s_{aJ}(E) >$ and $\langle s_a(E)\rangle$ denote the average of the spin dependent microscopic absorption cross section, and total absorption cross-section. Let us note here, that accounting for several level systems in the integral (12), it is useful to consider the mutual influence of those systems in respect to the effect of summation over J in the denominator. In our applications an acceptable approximation can be an over-determination of the parameters h like:

$$\overline{h_J^i} = b_i d\,\overline{\Sigma_{0J}}/\left[1 + b_i d\left(\langle\Sigma(E)\rangle - \langle\Sigma_{rJ}(E)\rangle\right)\right], \tag{22}$$

where $\langle\Sigma(E)\rangle$ is the average total cross section and $\langle\Sigma_{rJ}(E)\rangle$ the average resonance part of the total cross section. For a given J ($\langle\Sigma(E)\rangle = \Sigma_P + \sum_J \langle\Sigma_{rJ}(E)\rangle$) [4].

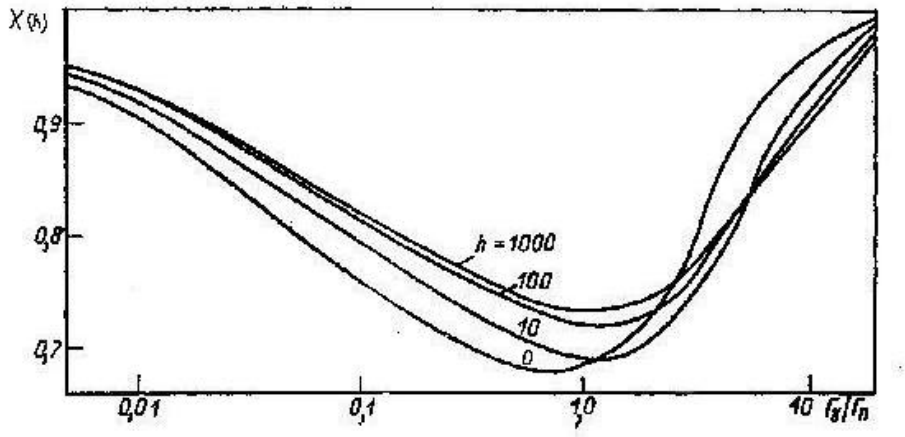

Figure 3. Fluctuation correction.

The target for the capture measurements discussed in paragraph 3 is a cylindrical disk with 80 mm diameter and a 0.5 mm thickness. This results in a ratio $R/d \geq 40$. The resulting values for the self-shielding coefficient C_2, calculated according to Eq. 21, agree with the results obtained with SESH (see Table 2). The total self-shielding correction (including C_1), calculated by SESH and MCNP, are given in the last two columns. Table 2 shows that the self-shielding and multiple scattering corrections deduced with MCNP are systematically larger than the SESH one's. The code SESH generates the Doppler broadened cross-section, but MCNP makes use of point-wise cross sections which are Doppler and resolution broadened. The resolution broadening may remove any possible resonance structure from the cross section and so from the transmission at the given energy. In the past, very high *Fe* transmission measurements (~390m) carried out at GELINA [17] proved that in a given energy interval the observation of structures in the transmission increases the average neutron transmission, i.e. reduces the self-shielding correction. This is also pointed out in Ref. [18]. We used the results from SESH to correct the experimental capture data of Ref. [9].

Table 2. Calculated values of $\bar{f}_0$ and C_2

E / keV	<σ> (barn)	σ_p (barn)	$\bar{f}_0$	Eq.21 C_2	SESH C_1	SESH C_2	SESH C_1+C_2	MCNP C_1+C_2
4-6	16.28	9.98	.0164	0.0345	0.9616	0.0328	0.9944	1.0410
6-8	15.45	9.95	.0163	0.0354	0.9615	0.0270	0.9885	1.0403
8-10	14.87	9.86	.0162	0.0359	0.9620	0.0409	1.0029	1.0400
10-15	14.24	9.75	.0160	0.0366	0.9656	0.0303	0.9959	1.0390
15-20	13.70	9.63	.0158	0.0367	0.9693	0.0364	1.0057	1.0370
20-30	13.22	9.46	.0155	0.0364	0.9748	0.0355	1.0103	1.0362
30-40	12.79	9.25	.0152	0.0361	0.9783	0.0340	1.0123	1.0360

2.4 Integral Form for $C_2(d)$

In the FF and NR approximation the coefficients $C_2^J(d,E)$ can also be obtained directly from the self-shielding coefficient at first collision $C_1^J(d)$. $P_0(x)$ may be written in the form:

$$P_0(x) = \int_1^\infty \frac{dt}{t^3} \int_0^t (1 - e^{-xt'}) dt', \quad (x = d\Sigma). \tag{23}$$

By substituting this expression in the relation for $C_1^J(d)$ (8) we obtain:

$$C_2(d) = f_0 \int_1^\infty \frac{dt}{t^3} \int_0^t t' C_1(dt') dt'' = f_0 \frac{1}{2} \left[\frac{1}{d^2} \int_0^d t dt C_1(t) + \int_d^\infty \frac{dt}{t} C_1(t) \right] \tag{24}$$

with

$$C_1(t) = \frac{1}{t}\int_0^t T_a(t')dt\,, \quad \text{and} \quad T_a(t') = \int \Sigma_a e^{-\Sigma t'} dE \,/\, \int \Sigma_a dE\,. \tag{25}$$

The function $T_a(t)$ can be obtained experimentally e.g. from self-indication methods as in Ref. [19]. For separated resonances it can also be calculated by [2, 4]:

$$T_a^{\,l}(t) = T_a^{\,l}(\Sigma_{0\,l}\,t, \Sigma_p t) = e^{-\Sigma_p t} e^{-\Sigma_{0l}/2} I_0(\Sigma_{0l}\,t/2)\,. \tag{26}$$

with I_o the Bessel function. Here Doppler broadening and interference in the scattering cross section are not accounted for. But, an approximate solution to include these effects is obtained by a corresponding over-determination of the parameters in (26): $\Sigma_p \to \Sigma_m$ (minimal cross section in the resonance), $\Sigma_{0\,l}(E) \to \Sigma_{0\,l}(E)\Psi(0, V_l)$. The expression (24) may be transformed by:

$$C_2(d) = f_0\left[C_1(d) + \frac{1}{2}\int_d^\infty \frac{dt}{t} T_a(t) - \frac{1}{2d^2}\int_0^d t T_a(t) dt\right] \tag{27}$$

3. EVALUATION OF THE AVERAGE RESONANCE PARAMETERS FOR ^{232}TH IN THE ENERGY REGION (4-40) KEV

In the unresolved resonance region only statistical modelling can reveal the resonant cross section structure, and accurately describe the average cross-section and their functionals in all energy intervals. Various schemes for the calculation of resonance-averaged cross sections in the URR are known [18]. They are mainly based on the Hauser-Feshbach formula. Since the fine structure is described in a single level Breit-Wigner approximation, such a scheme is in principle only valid for isolated resonances. Several procedures have been proposed to account for a significant resonance level overlap within the Hauser-Feshbach formalism. However, these schemes do not supply general analytical expressions for resonance-averaged cross-section functionals. They have to be calculated by Monte-Carlo simulations.

The model proposed in Ref. [8] not only provides the resonance-averaged cross sections but also their functionals. The model is based on the idea of introducing the characteristic function of the R-matrix element distribution. For the parameterisation of the cross-section the Reich-Moore R-matrix approximation is used. Applying this model, reliable average resonance parameters can be deduced from transmission, capture and self-indication measurement data obtained in the URR. To investigate the discrepancies (Fig.4) between the average capture cross-section for ^{232}Th(n,γ) reported in Ref. [9] and [20], we analysed the GELINA capture data [9] together with the results of the self-indication measurements of Ref. [10].

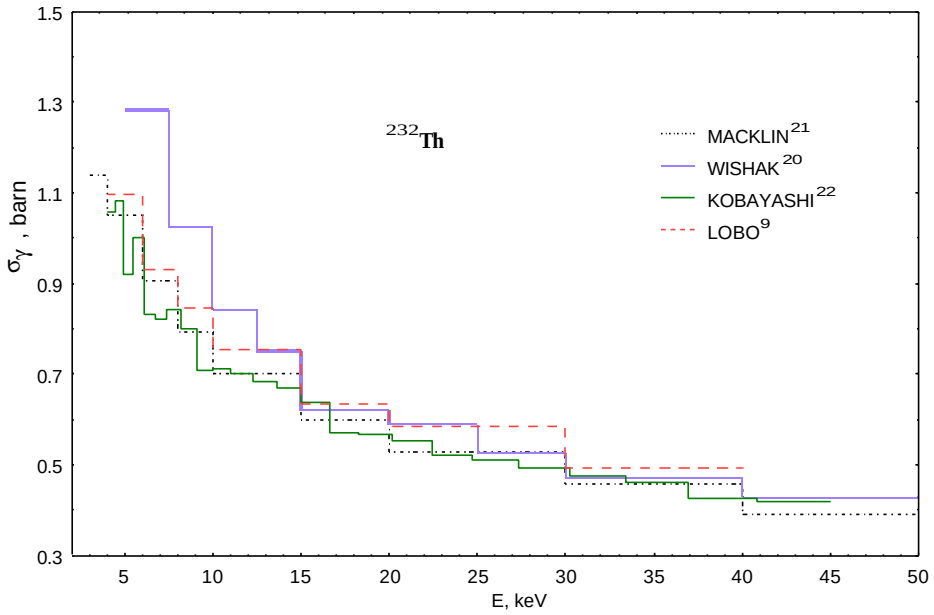

Figure 4. The experimental cross-section s_c for neutron capture for ^{232}Th in the energy range (4-50) keV.

3.1 Application of the characteristic function for the statistical modelling of cross sections in the URR

Applying the Reich-Moore R-matrix formalism, the total and partial cross-sections can be expressed in terms of real resonance parameters. In this approximation and in the case of single channel scattering in competition with many channels for neutron capture, the R-matrix becomes:

$$R_{nn}(E) = \sum_{l} \frac{g_{ln}^{2}}{(E_l - E - i\frac{\Gamma_{lg}}{2})} \qquad (28),$$

being E_l related to the resonance energy, g_{ln} the energy independent reduced neutron width amplitude and Γ_{lg} the total radiation width. The latter can be considered as a constant ($\Gamma_{\lambda\gamma} = \overline{\Gamma}_{\gamma}$). In the resolved resonance region, with a limited number of resonances, the reduced R-matrix is defined through the complete set of resonance parameters. In the unresolved resonance region only parameters averaged over many resonances can be extracted: the average reduced neutron width $\overline{\Gamma}_n$, the average radiation width $\overline{\Gamma}_g$, and the mean level spacing $\overline{D}$. These parameters obey well-known statistical distribution laws. The reduced resonance amplitude follows the Porter-Thomas distribution, whereas the level spacing follows the Wigner distribution. In Ref. [8], the average resonance parameters together with their statistical distributions are used to construct the characteristic function F of the R-matrix elements distribution. Using this characteristic function it is possible to obtain a set of resonances to

parameterise the cross-sections in the URR, similar to the parameterisation of the cross sections in the resolved resonance region.

For the R-matrix elements $R_{nn}(e)$

$$R_{nn}(e) = s\sum_{l}\frac{x_l}{e_l - e - iy} \tag{29}$$

with $s = (p\bar{g}_n^{-2})/(\overline{D})$, $y = (p\overline{\Gamma}_g)/(2\overline{D})$, $e = pE/\overline{D}$, $e_l = pE_l/\overline{D}$, and $x_l = g_{ln}^2/\bar{g}_n^2$, the characteristic function F in the interval ΔE is defined by:

$$F(g,b,y) = \frac{\overline{D}}{p\Delta E}\int_{\Delta E} de \prod_l \int P(x_l)dx_l \int Q(e_l)de_l \exp\left[x_l \frac{ib(e_l - e) - gy}{(e_l - e)^2 + y^2}\right] \tag{30}$$

The number of resonances considered in the interval are given by $\Delta E = N\overline{D}$. The free parameters γ and β are connected with the neutron strength function s, $P(x_l)dx_l$ denotes the Porter-Thomas distribution of the neutron widths, and $Q(e_l)de_l$ is the Wigner distribution for the resonance spacing. The F-function (Eq.27) contains the full information to describe in average the resonant cross section structure in the interval ΔE.

Two main problems arise in the calculation of the R_{nn}-matrix, when significant resonance interference is present in URR:

(i) the contribution of resonances which are not accounted for in the λ-summation, and
(ii) the influence of energy regions which are not included in ΔE.

To account for these effects a periodic structure of the resonant cross sections with a certain periodicity ($0 < e < pN$) is proposed. The infinite summation over l in (Eq. 27) is reduced to a finite one:

$$R_{nn}^m(e) = \frac{s}{N}\sum_{l=0}^{N-1} x_l ctg\left[(e_l - e - iy)/N\right] \tag{31}$$

It is proved that the "model" $R_{nn}^m(e)$-matrix fulfils the basic requirements for a correct description of the real resonant cross-section structure when averaged in ΔE. By fitting the "model" characteristic function F^m of $R_{nn}^m(e)$ to the "exact" function F (Eq.28) various sets of $2N$ resonance parameters (e_l, x_l) of $R_{nn}^m(e)$ can be obtained. Each of them is capable to describe the resonant cross section for a wide variety of nuclei in a certain interval ΔE. In the interval ($0 < e < pN$) point-wise cross sections can be calculated via the $R_{nn}^m(e)$-matrix and used to estimate for a finite interval ΔE the average total and partial cross-sections and their related functionals.

By fitting the experimental with the theoretical data average, resonance parameters can be obtained from transmission, capture and self-indication measurements in the URR. To perform such a fitting procedure the program MINUIT [23] may be used.

3.2 Evaluation of average resonance parameters for ^{232}Th in energy range (4-40) keV.

Average resonance parameters for ^{232}Th, in the URR below the inelastic scattering threshold, are deduced by fitting experimental average capture data with theoretical expressions. The measurements were carried-out at the 14.5 m flight-path of the GELINA spectrometer of the IRMM (B). The free parameters in the fitting procedure are: the average reduced neutron width ($\overline{\Gamma}_n^l$), the average radiation width ($\overline{\Gamma}_g$), the mean level spacing ($\overline{D}$) and the effective scattering radius (R'). The parameters $\overline{\Gamma}_n^l$, $\overline{\Gamma}_g$ and $\overline{D}$ are adjusted only for s- and p-wave neutrons. The radius R' is considered to be independent of the orbital angular momentum of the incoming neutron. The average parameters for d-wave neutrons are fixed and taken from JENDL 3.2. The resulting parameters and the initial values from JENDL 3.2 are summarised in Table 3. To verify the results, we also performed a fit of the GELINA data together with the data from self-indication measurements of Ref. [10]. The average parameters from this simultaneous analysis are given in the last column of Table 3 and are in good agreement with the data deduced from the capture measurements. The resulting average capture cross-section also deviates with about 40% from the data reported in Ref. [20], confirming the conclusions made in Ref. [9].

Table 3. Average resonance parameters for ^{232}Th in (4-40 keV).

		JENDL 3.2	Fitted average resonance parameters	
			$\overline{s}_{g\,\mathrm{exp}}$	$\overline{s}_{g\,\mathrm{exp}}$, $f_{g\,\mathrm{exp}}$
$\overline{\Gamma}_n^l$ / meV	l=0, J^π=0.5	1.730	1.90	1.83
	l=1, J^π=0.5	3.650	3.91	3.69
	l=1, J^π=1.5	1.807	1.95	1.84
	l=2, J^π=1.5	0.922		
	l=2, J^π=2.5	0.616		
$\overline{\Gamma}_g$ / meV	l=0, J^π=0.5	21.20	25.37	26.19
	l=1, J^π=0.5	21.20	24.24	25.22
	l=1, J^π=1.5	21.20	24.24	25.22
	l=2, J^π=1.5	21.20		
	l=2, J^π=2.5	21.20		
$\overline{D}$ / eV	l=0, J^π=0.5	18.464	18.03	18.42
	l=1, J^π=0.5	18.464	18.03	18.42
	l=1, J^π=1.5	9.217	9.02	9.21
	l=2, J^π=1.5	9.217		
	l=2, J^π=2.5	6.159		
R' / fm	l=0,1,2	10.010	8.94	8.99

4. CONCLUSIONS

The characteristic function statistical model, proposed in Ref. [7,8], is presented and applied to deduce average resonance parameters in the unresolved resonance region for ^{232}Th. Average parameters are obtained from a simultaneous analysis of average capture and self-indication data. The resulting average capture cross-section confirms the results presented by Lobo et al. [9], and does not show discrepancies with evaluated data as large as the ones reported in Ref. [19].

To correct experimental capture data for self-shielding and multiple scattering effects an analytical solution is proposed. In contrast to other analytical solutions, such as the one proposed by Dresner, we formally include the effect of resonance and potential scattering interference, and also take into account the Doppler broadening of the resonances. In addition, we propose a procedure to deduce the C_2 coefficient directly from the C_1 coefficient even in case of significant level interference (e.g. for fissile nuclei). This offers the possibility to estimate the self-shielding and multiple scattering corrections from experimental data.

REFERENCES

1. M. Case, P. F. Zweifel, *Linear Transport Theory*, Addison–Wesley Pub. Co, London (1967).
2. L. Dresner, "Resonance self-shielding in the measurement of radiative capture cross sections", *Nucl. Instr. Meth.*, **16,** p. 176 (1962); L. Dresner, *Resonance Absorption in Nuclear Reactors*, Pergamon Press, NY (1960).
3. G. I. Marchuk, *Methods for nuclear reactors calculation*, Gosatomizdat, Moscow (1961).
4. A. A. Lukyanov, *Slowing down and absorption of resonance neutrons*, Atomizdat, Moscow (1974).
5. J. F. Briestmeister, *MCNP: A General Monte Carlo N-Particle Transport Code, Version 4C*, LA-13709-M (2000).
6. F. H. Froehner, *Report GA-8380*, Gulf General Atomic (1968).
7. N. Koyumdjieva, N. Janeva and A. A. Lukyanov, Z. Phys. **A253**, p. 31 (1995).
8. N. Koyumdjieva, N. Janeva and K. Volev, "Validation of the characteristic function model for the unresolved resonance region", *Nuclear Science and Engineering*, **173,** pp. 194-205 (2001).
9. G. Lobo, F. Corvi, P. Schillebeeckx, N. Janeva, A. Brusegan, P. Mutti, "Measurement of the Th neutron capture cross-section in the region 5 keV-150 keV", *Int. Conf. Nuclear Data for Science and Technology*, Tsukuba, Japan, Oct., 7-12, 2001.
10. H. Oigawa, Y. Fujita, K. Kobayashi, S. Yamamoto, I. Kimura, "Self-shielding factors for neutron capture reactions of uranium-238 and thorium-232 in energy range of 1~35 keV", *Journal of Nuclear Science and Technology*, **28**, pp. 879-893 (1991).
11. M. Moxon, *REFIT2: A least Squares Fitting Program for Resonance Analysis of Neutron Transmission and capture Data*, NEA-0914/02 (1989).
12. N. Larson, *Updated Users' Guide for SAMMY: Multilevel R-matrix Fits to Neutron Data Using Bayes' Equations*, ORNL/TM-9179/R5, Oak Ridge National Laboratory, Oak Ridge, TN (2000).

13. N. Larson and K. Volev, "Validation of the multiple-scattering corrections in the analysis code SAMMY", *PHYSOR 2002,* Seoul, Korea, October 7-10 (2002).
14. R. L. Macklin, "Resonance self-shielding in neutron capture cross section measurements", *Nucl. Instr. Meth*., **26,** p. 213 (1964).
15. *Handbook of Mathematical Functions*, Ed. M. Abramowitz and I.A. Stegun, NBS Publ., (1964).
16. L. P. Abagyan et al., *Diffusion of resonance neutrons in homogeneous media, Bulletin of NDC,* Atomizdat, Moscow (1968).
17. K. Berthold , C. Nazareth, G. Rohr, H. Weigmann, "Very High Resolution Measurements of the Total Cross Section of Natural Iron", *Int. Conf. Nuclear Data for Science and Technology*, Gatlinburg, Tennessee US, May 9-13 (1994).
18. F. Fröhner, "Evaluation and Analysis of Nuclear Resonance Data", JEFF Report 18, (2000).
19. N. Janeva, S. Toshkov, G. V. Muradyan, Yu. V. Grigorjev, G. Georgiev, I. Sirakov, V. G. Tishin and Yu. S. Zamjatnin, "A setup for precise measurement of resonance neutron capture by self-indication", *Nucl. Instr. and Meth. in Phys. Res.* **A313,** p. 266 (1992)
20. K. Wisshak, F. Voss and F. Kappeler, "Neutron capture cross section of ^{232}Th", *Nuclear Science and Engineering*, **173,** p. 183 (2001).
21. R. L. Macklin and R. R. Winters, "Stable isotope capture cross sections from the Oak Ridge Electron Linear Accelerator", *Nuclear Science and Engineering*, **78**, p. 110 (1981).
22. K. Kobayashi, Y. Fujita and N. Yamamuro, "Measurement of the neutron capture cross section of Th-232 from 1 keV to 408 keV", *Journal of Nucl. Sci. and Techn.*, **18,** p. 823 (1981).
23. *MINUIT – Function Minimization and Error Analysis, Version 94.1*, CERN Program Library Long Writeup D506.